International Journal of Applied Pharmaceutics

ISSN- 0975-7058 Vol 18, Issue 1, 2026

Original Article

MIRTAZAPINE LOADED PRONANOMICELLES: PREPARATION AND CHARACTERIZATION

AHMED IBRAHIM AHMED, NAWAL AYASH RAJAB*

Department of Pharmaceutics, College of Pharmacy, University of Baghdad, Baghdad, Iraq
***Corresponding author: Nawal Ayash Rajab; *Email: dr.nawalayash@copharm.uobaghdad.edu.iq**

Received: 11 Aug 2025, Revised and Accepted: 24 Oct 2025

ABSTRACT

Objective: The aim of this work was to prepare mirtazapine-loaded self-assembled micelles using soluplus®, solutol®HS15 and TPGs to enhance mirtazapine solubility and thus oral bioavailability.

Methods: MTZ nanomicelles were produced by the thin-film hydration method using different polymers in different ratios to prepare stable MTZ nanomicelles, where the soluplus® nanomicelles formula in different ratios was F1 to F4; soluplus® in combination with TPGS to stabilize the nanomicelles formula was formulated in different ratios as in F5 to F10; and soluplus® in combination with SolutolHS 15 as in F10 to F14. The most stable formula is further investigated with particle size, polydispersity index, drug loading, entrapment efficacy, and *in vitro* release, and then the selected formula is statistically further investigated with FTIR, DSC, and FESEM.

Results: The particle size of the prepared formula ranged from 57 nm for F4 (1:10 of MTZ: soluplus®) to 78 nm for F8 (1:8:4 of MTZ: soluplus®: TPGS); the EE% ranged from 85% to 90%; FTIR analysis suggested no chemical interaction; FESEM showed spherical nanomicelles in Nano size; and DSC showed the transition of the drug to an amorphous form due to MTZ entrapment with in nanomicelles.

Conclusion: Mirtazapine-loaded Soluplus® micelles alone and in combination, first with TPGS and second with Solutol HS 15 by the thin-film hydration method show uniform distribution of particle size, PDI, and enhancement in the *in vitro* release of the drug.

Keywords: Mirtazapine, Nanomicelles, Thin-film hydration method, Soluplus®, Solutol HS 15

DOI: https://dx.doi.org/10.22159/ijap.2026v18i1.56474 Journal homepage: https://innovareacademics.in/journals/index.php/ijap

INTRODUCTION

To enhance the solubility and augment the stability and oral bioavailability of weakly water-soluble compounds, many techniques have been proposed. Nano-micelles are utilized as effective agents for encapsulating pharmaceuticals with low water solubility. The core-shell architecture of micelles inhibits the infiltration and existence of water within its inner core. This essential characteristic of micelles establishes an optimal environment for the encapsulated medicine relative to the free drug. Several advantages of micelles as medication transporters include simplicity [1].

A number of technological methods, such as chemical modification, co-solvency, cyclodextrin complexation, micellization, microemulsion, micronization, mucoadhesive microspheres, nanoemulsion, nanoparticles, nanosuspensions, self-emulsifying systems, and solid dispersion, have been used to enhance the solubility of poorly aqueous soluble drugs [2].

Polymeric micelles with a core-shell structure and particle size less than 100 nm display many privileges, including encapsulation of hydrophilic or hydrophobic anticancer drugs, high-efficiency drug loading, long systemic circulation time, and functionalizing with different targeting moieties [3].

The amphiphilic molecules that make up micelles typically self-assemble into structured supramolecular assemblies in water. Depending on the molecular weights of the blocks that comprise the core and corona, micelles can be created in a variety of shapes and sizes, ranging from spherical to cylindrical to star-shaped, and everything in between. A critical micelle concentration (CMC) is the concentration at which self-assembly begins to occur [4].

For typical micellar structures, hydrophobic interactions of core-forming blocks provide the driving force for self-assembly and maintenance of supramolecular assembly. Because the corona-forming block dissolves in water, micelles can dissolve in water as well. Nanocarriers can be used to increase the water solubility of hydrophobic compounds by taking advantage of their hydrophobic core [5].

Nanomicelles can be divided into three broad categories, i. e., polymeric, surfactant, and polyionic complex (PIC) micelles. In order to choose the best nanomicelle carrier, several factors must be considered, including the physicochemical properties of the drug molecule, interactions between the drug and polymers or surfactants, the location of action, the rate of drug release, biocompatibility, and physical stability [6zzz].

Mirtazapine is an antidepressant utilized for the management of moderate to severe depression, with a molecular formula of C17H19N3. This medicine has a bioavailability of 50% owing to first-pass metabolism, possesses a high protein binding rate of 80%, and has an extended half-life ranging from 20 to 40 h [7, 8]. Mirtazapine is substantially insoluble in water, with a logarithm partition coefficient (octanol-water) of 2.9, signifying considerable hydrophobicity [9]. The aim of this research was increasing the solubility of mirtazapine by encapsulation it in polymeric micelles as drug delivery Nano-carriers using different amounts and combinations of amphiphilic polymers that may be lead to the enhancement of the drug bioavailability.

MATERIALS AND METHODS

Materials

Mirtazapine was purchased from Macklin, China. soluplus® was purchased from BASF, Germany. D-α-tocopheryl polyethylene glycol 1000 succinate was purchased from Hangzhou, Hyperhem, china. Solutol HS-15 was purchased from Picasso, China. Methanol was purchased from Chem-Lab, Belgium.

Method

Preparation of mirtazapine loaded nanomicelles

Mirtazapine nanomicelles were produced by the thin-film hydration method (table 1). All components (mirtazapine and polymers) were solubilized in 20 ml of methanol. The solutions were subsequently evaporated at 150 rpm and 60 °C for 30 min using a rotary evaporator under a vacuum of 7.4 kPa, resulting in the formation of a thin layer. Subsequently, the thin layer was hydrated with 10 ml of deionized water, while the nanomicelles dispersion was subjected to sonication for 5 min before being magnetically agitated for 60 min at 500 rpm [10, 11].

Table 1: Compositions of MTZ nanomicelles

Formula code	MTZ mg	Ratio (drug: polymer: stabilizer)	Soluplus® mg	TPGS mg	Solutol HS 15 mg
F1	7.5	1:4	30	_	_
F2	7.5	1:6	45	_	_
F3	7.5	1:8	60	_	_
F4	7.5	1:10	75	_	_
F5	7.5	1:4:2	30	15	_
F6	7.5	1:4:4	30	30	_
F7	7.5	1:8:2	60	15	_
F8	7.5	1:8:4	60	30	_
F9	7.5	1:6:4	45	30	_
F10	7.5	1:6:6	45	45	
F11	7.5	1:4:2	30	_	15
F12	7.5	1:4:4	30	_	30
F13	7.5	1:8:2	60	_	15
F14	7.5	1:8:4	60	_	30

Characterization of MTZ nano-micelles

Micelles size determination and polydispersity index (PDI)

The Zetasizer, manufactured by Malvern Instruments Ltd in the United Kingdom, was used to determine the nanomicelles size and polydispersity index (PDI) of all the formulations that were prepared. This dynamic light scattering apparatus measures the amount of light molecules scattering as a time function at a constant temperature of 25 °C and a scattering angle of 90° [12, 13].

Zeta potential measurement

The electrophoretic mobility of a prepared formula was assessed using the Malvern Zetasizer Nano ZS device (Malvern Instruments, Worcestershire, UK). This measurement was subsequently translated to zeta potential, which indicates the extent of repulsion among charged particles and evaluates the stability of the created dispersion. The sample was placed into an electrophoretic cell by applying an electric field with a voltage of 15.2 V/cm [14].

Drug loading content (DL %) and encapsulation efficiency (EE %)

The entrapment efficiency percentage (EE %) and drug loading percentage (DL %) that correspond to the percentage of MTZ entrapped were indirectly measured based on the free MTZ concentration in the Nano-micelles. A free drug amount not entrapped was identified through the measurement of free drug using the ultrafiltration process. A total of 3 ml of MTZ solution of the Nano-micelles was spun at 5,000 rpm (279 g forces) for 30 min after being put into the upper chamber of an Amicon Ultra centrifugal tube with a molecular cut-off size of 10 KDa. Using a UV-vies spectrophotometer set at 294 nm, we determined the free drug content of MTZ in the ultrafiltration after the necessary dilution [15]. And then using these equations.

$$DL\% = \frac{(total\ drug\ in\ formula}{total\ conc\ of\ formula} \times 100\% \quad \text{.....Eq2 [16]}$$

$$EE\% = \frac{(total\ drug\ in\ formula - amount\ of\ free\ drug)}{total\ drug\ in\ formula} \times 100\% \quad \text{..Eq1 [17]}$$

***In vitro* release study**

With the using of a dialysis bag along with a dialysis membrane from the MYM biological technology firm in the USA (MWCO: 8-14 kD), *in vitro* release of MTZ from nanomicelles along with pure MTZ powder was studied. Phosphate buffer with a pH of 6.8 and a dissolution medium of 500 ml was employed as a release medium for the selected formula. A USP apparatus for dissolution (RIGGTEK, Dissilio TX8, Germany) was utilized to keep the systems at 37 °C stirred at a speed of 100 rpm. After 5, 10, 15, 20, 30, 45, 60, 90, 120, 150, and 180 min, a sample of 4 ml from the outer medium was withdrawn and replaced with a fresh medium of the dissolution. Following the measurement of the absorbency at 290 nm using a UV spectrophotometer, the samples' triplicate test was performed [18].

The results acquired from the dissolution studies were statistically validated using a similarity factor (*f2*). The *f2* was used to consider similar dissolution profiles (equation below).

$$f_2 = 50 \times \log \{[1+(1/n) \sum_{j=1}^{n} w |R_j - T_j|^2]^{.5} \times 100\}$$

To ensure sink condition conformation, by using 4 ml of nanomicelles preparation that contain equal to 3 mg in 500 ml of phosphate buffer and the concentration well be in this media equal to 0.006 mg/ml, that compared to solubility of MTZ in phosphate buffer (0.0737 mg/ml), that mean 500 ml enough volume for dissolution Here, (n) is the total number of times that dissolution has occurred. The dissolution values from the reference and test samples at time t are denoted by (R), (T), respectively. When the $f_2$values are between 50 and 100, the two dissolution profiles are considered similar [11].

The *in vitro* release kinetics of MTZ of the prepared nanomicelles formulation was evaluated to understand the drug release behavior. The correlation coefficient (R^2) was determined from the linear regression of these plots.

Fourier transforms infrared spectroscopy (FTIR)

Pure MTZ, physical mixture with ratio (1:1), and Nano-micelles formulations were analyzed by using a Fourier transform infrared spectrophotometer (Shimadzu 4100, Japan). The sample were mixed with potassium bromide and compressed into disks using hydraulic press before scanning from 4000 to 400 cm^{-1} [19].

Field emission scanning electron microscope

The morphology of the MTZ Nano-micelles formulation was studied using a field emission scanning electron microscope (FESEM) developed by Hitachi, Japan, specifically the FESEM S-4160. The examination of samples with the Field Emission Scanning Electron Microscope (FESEM) relies heavily on the sample preparation process. The level of care put into preparing the sample determines the quality of the FESEM image. To prepare the sample, we carefully collected the Nano-micelles, fixed them so that their structure would remain intact, dried the formula to remove any remaining water, and then coated them with a conductive material called platinum [20].

Differential scanning calorimetric (DSC)

A heat transfer measurement instrument (DSC-60; Shimadzu, Japan) produced and analysed thermograms for three sample types: (1) pure MTZ, (2) a physical mixture of MTZ and excipients, and (3) the selected nanomicelles formulation. The temperature was raised from 25 to 300 °C at 10 °C/min, with a nitrogen flow rate of 50 ml/min [21].

Stability assessment on storage

To evaluate the long-term physical and chemical stability of AMS-loaded NMs, samples were stored in sealed glass vials under two conditions: ambient temperature (25 °C) and refrigerated (4 °C) for 90 d. Post-storage, formulations underwent comprehensive analysis, including drug content quantification, P. size measurement, PDI, DL, and Visual inspection for precipitation events.

Solubility determination of MTZ-NM dispersion

The saturation solubility of selected dispersion, to be optimized, was determined in phosphate buffer pH 6.8 by adding approximately 1.5

ml of dispersion to a 2 ml of phosphate buffer pH 6.8 in centrifugation tube. The tubes were shaken at 25 °C for 48 h to ensure saturation. After reaching equilibrium solubility, the clear supernatant was filtered through a 0.45-µm, properly diluted, and measured using a UV-spectrophotometer at its confirmed λ max, Triplicates of each experiment were conducted.

STATISTICAL ANALYSIS

The results were expressed as a mean value (±SD; n = 3), The one-way analysis of variance test was employed to assess the significance of differences among the findings derived from the examined formulations. The significance level was established at p = 0.05, with values below this threshold being statistically significant and those above regarded as statistically insignificant [22].

RESULTS

Micelles size and PDI

Particle size was ranged from 57.6 nm for F4 (MTZ: soluplus 1:10) to 77.33 nm in F3 formula (MTZ: soluplus 1:8) as shown in table 2 the P. S decrease as concentration of soluplus increase and PDI ranged from (0.03 to 0.3) as in table 2.

Table 2: Particle size, PDI, EE and DL

Formula	Particle size nm	PDI	EE%	DL%
F3	77.33±2.52	0.05±0.06	85.9±0.001	10.06±0.017
F4	57.67±3.6	0.035±0.041	90±0.01	8.23±0.013
F7	77.33±3.51	0.085±0.04	86.8±0.02	8±0.002
F8	78.34±4.04	0.144±0.012	87.8±0.014	7.65±0.011
F9	71.67±2.51	0.24±0.094	87±0.0012	8.04±0.015
F10	77.00±2.65	0.311±0.08	87.8±0.001	7.17±0.012
F12	73.67±4.23	0.130±0.01	86.8±0.011	10.08±0.02
F13	76.34±4.52	0.069±0.13	86.2±0.012	8.33±0.051
F14	75.00±4.00	0.07±0.02	89±0.011	7±0.0013

Results are given in mean±SD; n = 3

Drug loading content (DL%), Encapsulation efficiency (EE%) and zeta potential

The entrapment efficiency (EE) ranges from (85% to 90%) as shown in table 2. Zeta potential was measured for optimum formula, was equal to-7.10mv.

***In vitro* release study**

The drug release profile of nanomicelle formulations containing MTZ was compared with the pure drug using similarity and dissimilarity variables. The *in vitro* dissolution profiles showed dissimilarities, with *f2* values of pure drug versus nanomicelle formulation less than 50, meaning all successful nanomicelle formulas enhanced the dissolution of MTZ. The release study done in triplicate for each formula.

After fitting the *in vitro* release data into various kinetic models, the regression parameters obtained are shown in table 3. The best fit for the various models examined for the nanomicelles are graded in the order of first order with F_{max}>First order>Higuchi>zero order.

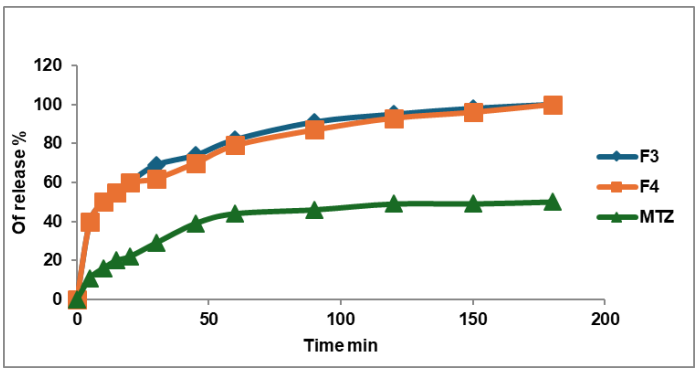

Fig. 1: Release profile of MTZ: soluplus®nanomicelles and pure drug in phosphate buffer with a pH of 6.8 and 37 °C ±1 °C, n = 3)

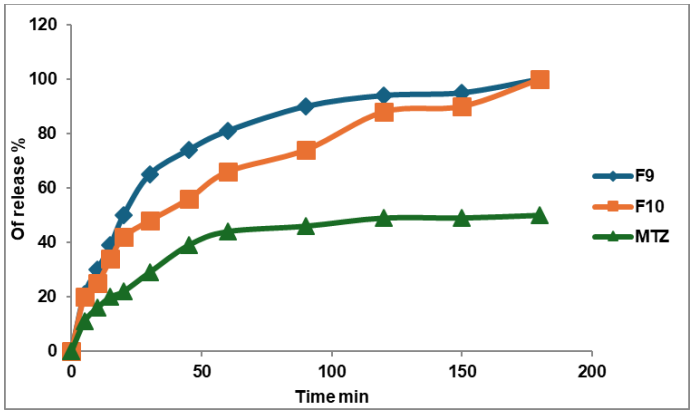

Fig. 2: Release profile of MTZ: soluplus®: TPGs nanomicelles and pure drug in phosphate buffer with a pH of 6.8 and 37 °C ±1 °C, (n = 3)

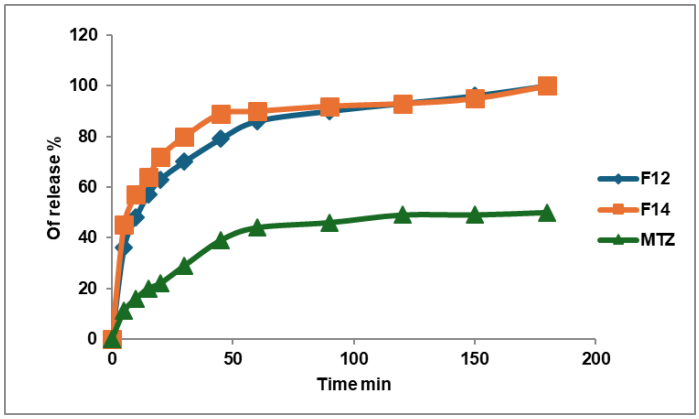

Fig. 3: Release profile of MTZ: soluplus®:Solutol HS nanomicelles and pure drug in phosphate buffer with a pH of 6.8 and 37 °C ±1 °C, (n = 3)

Table 3: Releas kinetic parameter of MTZ nanomicelles

Formula code	Zero order		First order		Higuchi		First order with Fmax		
	K_0	R_{seq}	K_1	R_{seq}	KH	R_{seq}	K_1	Rseq	F max
F3	0.772	-0.5122	0.047	0.8929	9.220	0.6834	0.061	0.9236	91.403
F4	0.754	-0.4624	0.042	0.8399	8.981	0.7000	0.061	0.8918	88.656
F7	0.753	0.2071	0.032	0.9884	8.807	0.8880	0.036	0.9935	95.555
F8	0.689	0.5413	0.020	0.9558	7.866	0.9812	0.024	0.9638	92.594
F9	0.771	-0.5731	0.050	0.9293	9.247	0.6523	0.063	0.9603	91.667
F10	0.788	-1.2828	0.072	0.9329	9.627	0.3440	0.090	0.9674	92.318
F12	0.385	0.2531	0.006	0.5786	4.492	0.8925	0.033	0.9912	89.589
F13	0.702	-0.5122	0.047	0.8929	8.320	0.8601	0.053	0.9732	85.969

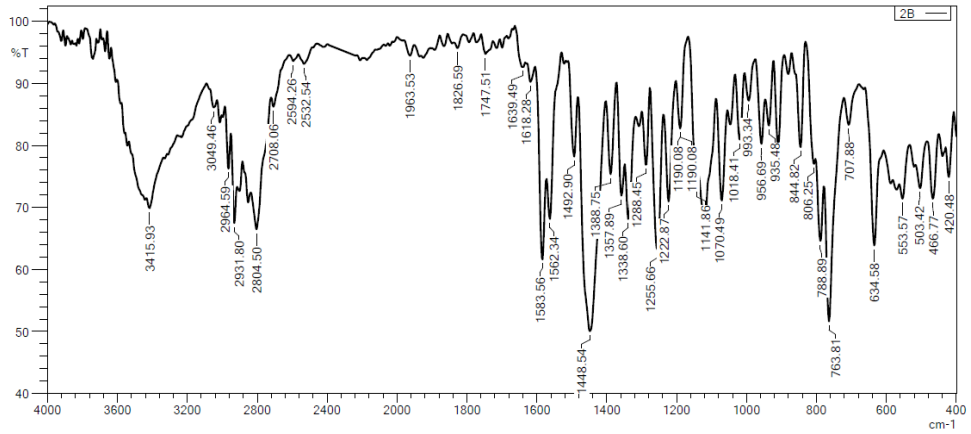

Fig. 4: FTIIR spectrum of mirtazapine powder

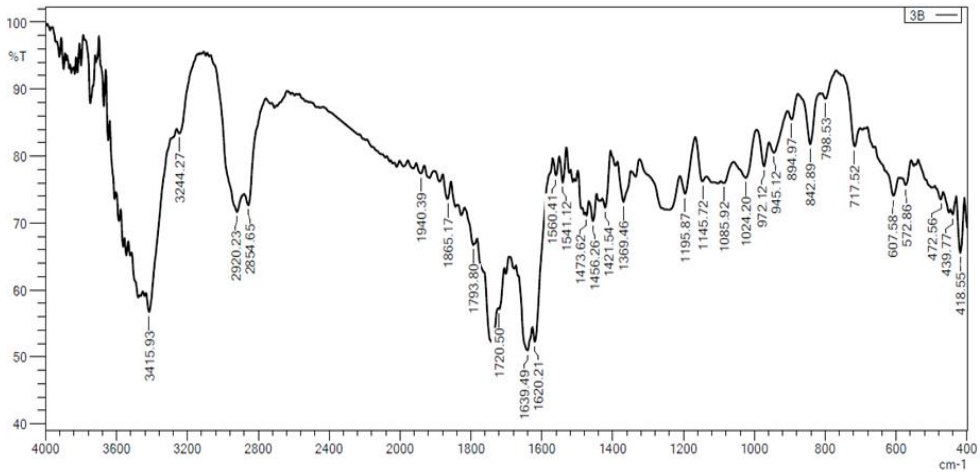

Fig. 5: FTIR spectrum of Soluplus® powder

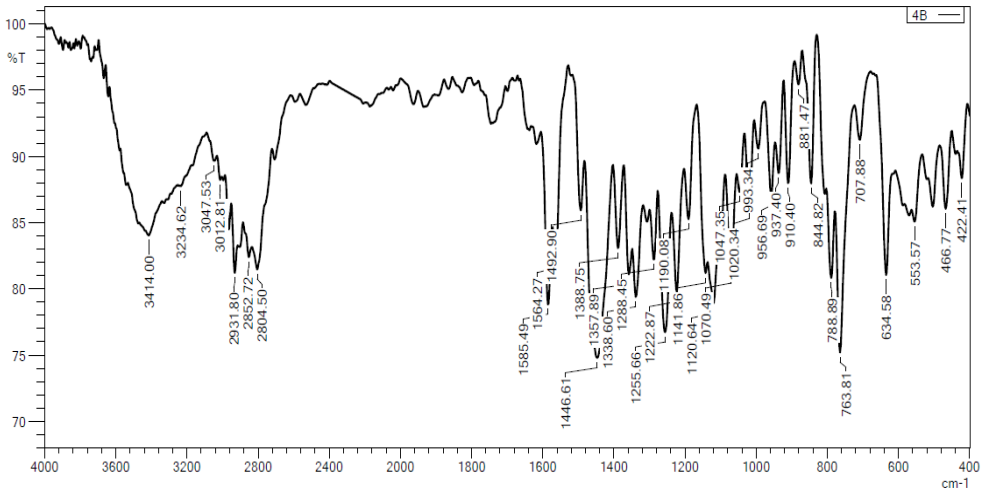

Fig. 6: FTIR spectrum of physical mixture (1:10 mirtazapine to soluplus® ratio)

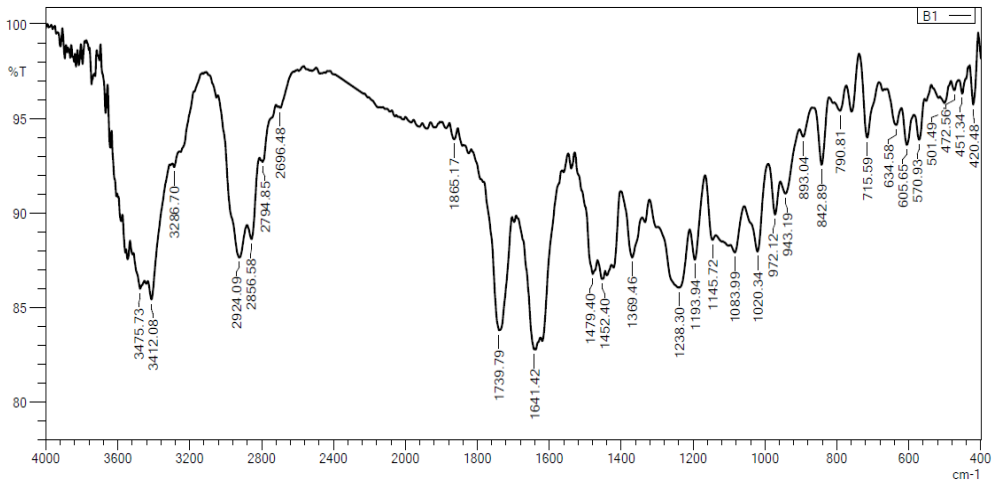

Fig. 7: FTIR spectrum of selected nanomicelles formula (F4)

Fourier transforms infrared spectroscopy (FTIR)

The FTIR analysis of the selected formula in fig. 7 shown definite absorption peaks of MTZ. This indicates that there was no significant chemical interaction [23, 11].

Field emission scanning electron microscope

FESEM fig. 8, shows the particle size in nanometer of selected formula F4 and the shape of micelles that composed of the outer layer shell and the inner core that entrap mirtazapine.

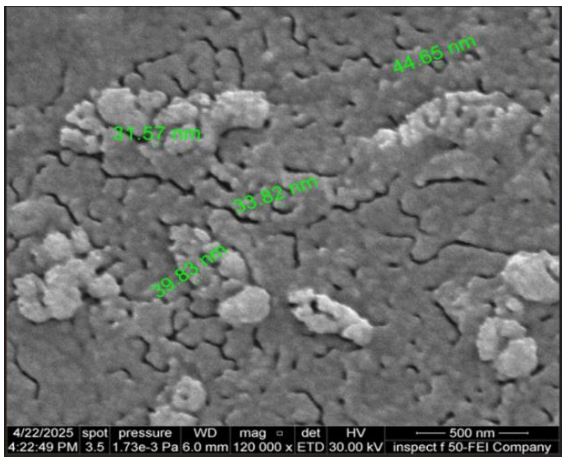

Fig. 8: FESEM of selected nanomicelles formula F4(scale pare in 500 nm and magnificent 120000X)

Differential scanning calorimetric (DSC)

DSC thermograme was performed to investigate the phase transition of MTZ during the production of polymeric nanomicelles. For selected formula DSC thermogram show transition from crystalline to amorphous due nanomicelles formation as in fig. 12, The result demonstrated that MTZ was well dispersed in the nanomicelles as an amorphous form [24-26].

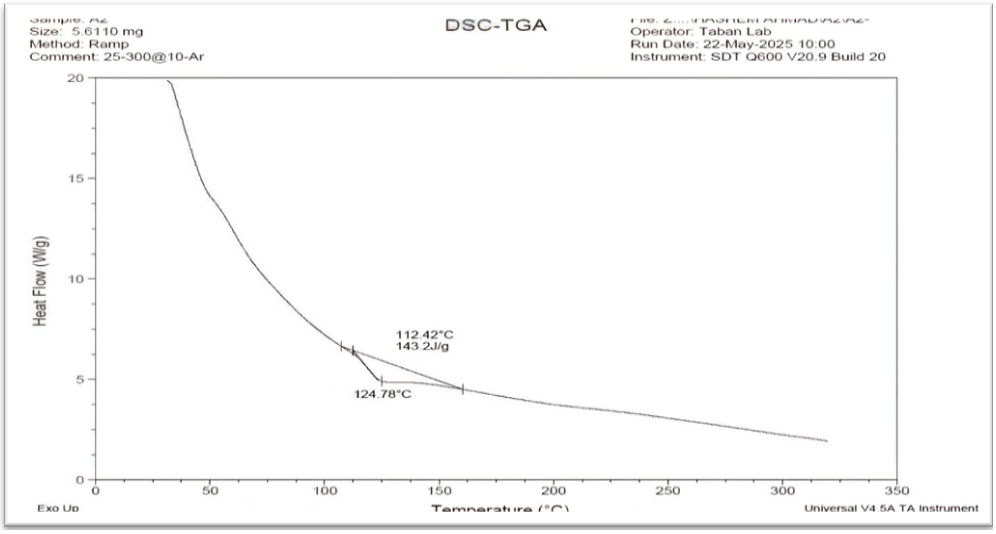

Fig. 9: DSC thermogram of MTZ

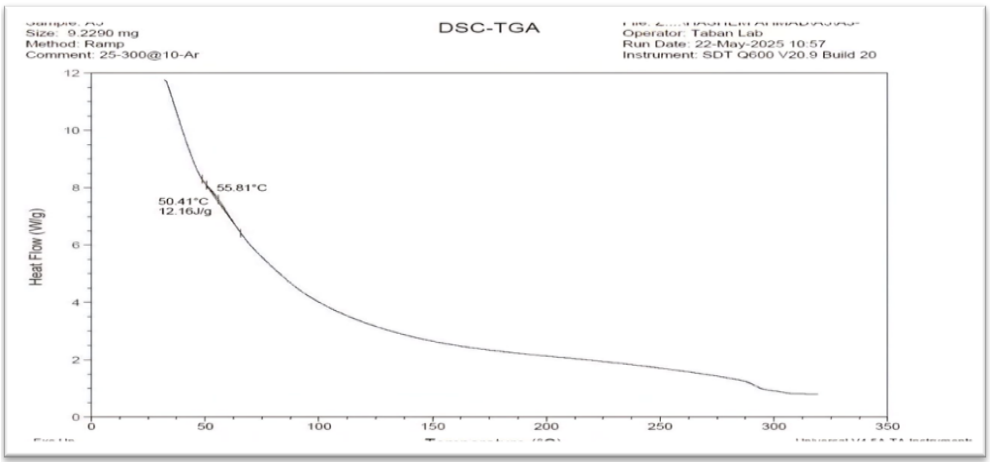

Fig. 10: DSC thermograms of Soluplus®

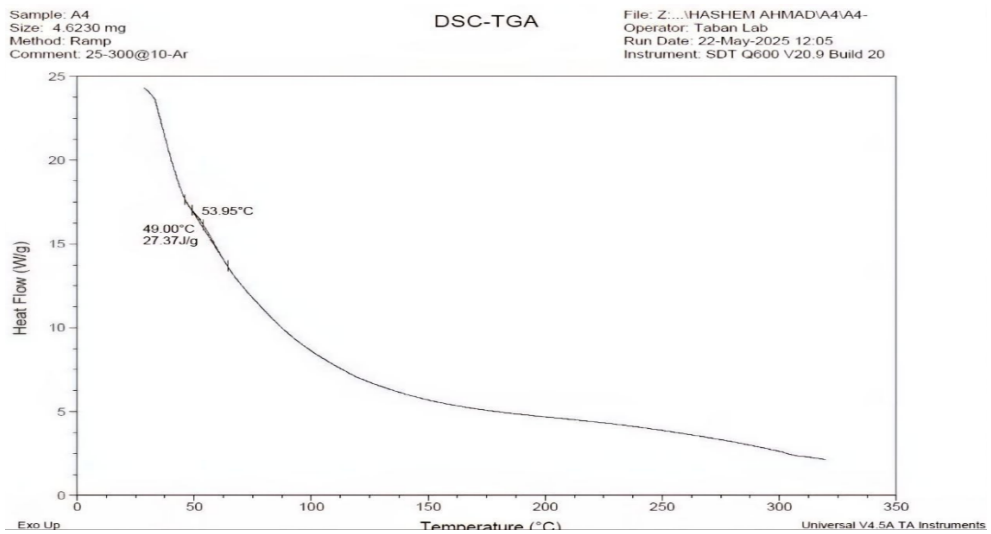

Fig. 11: DSC thermogram of MTZ-Soluplus®(1:10) physical mixture

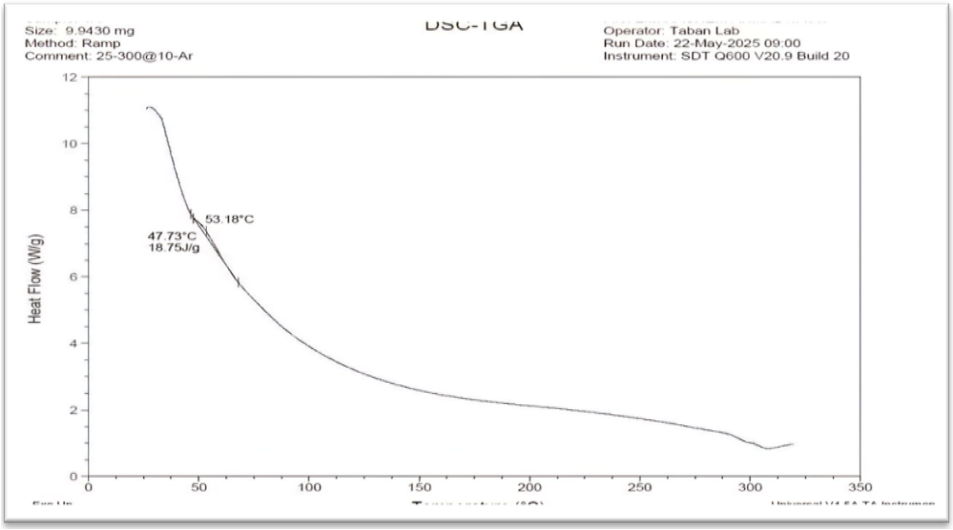

Fig. 12: DSC thermogram of selected nanomicelles formula (F4)

Stability study

The storage stability of the optimized MTZ-NM dispersion (F4) was evaluated over three months under two conditions: refrigerated at 4 °C and ambient temperature. Particle size was monitored using a Malvern Particle Size analyzer, while encapsulation efficiency (EE%) and content% % were determined spectrophotometrically at 294 nm. Additionally, a visual inspection was performed to detect any precipitation of MTZ. The stability data are summarized in table 3, which demonstrates that the PS and PDI remained consistently low and within the Nano scale range (<100 nm) across all conditions, indicating that the NM maintained their uniform size distribution and colloidal stability after 3 mo of storage at both refrigerated (4 °C) and room temperature (25 °C). The clear appearance without precipitation or turbidity further supports the physical stability of the formulation. The EE% values showed a minimal decrease (from 73% to 70%) after 3 mo at 25 °C, indicating negligible drug leakage or degradation. The drug content remained above 98% in all conditions, confirming excellent chemical stability and preservation of MTZ integrity during storage and dilution.

Saturated solubility of mirtazapine

The saturation solubility of MTZ shown in table 5, and solubility of optimum formula (F4), which show enhancement in solubility of MTZ.

Table 4: Stability parameter of F4 NM-dispersion

Storage condition	PS (nm)	PDI	EE%	Appearance	DL
4 °C after 3 mo	57.1±2.2	0.031 ±0.002	90.24± 3.6	Clear	10.9± 0.01
25 °C after 3 mo	60.09 ±3.4	0.039± 0.004	89.12± 2.4	Clear	9.7± 0.05

Results are given in mean±SD; n = 3

Table 5: Saturated solubility data of mirtazapine

Media for the solubility study	MTZ Solubility (mg/ml)	MTZ-NM dispersion solubility (mg/ml)
Phosphate buffer saline pH 6.8 (PBS)	0.737 ±0.04	2.3 ±0.03

Results are given in mean±SD; n = 3

DISCUSSION

Micelle size and distribution (PDI) were characterized using dynamic light scattering (DLS). At low Soluplus® concentrations, as in formulas F1 (1:4) and F2 (1:6), micelles formed but precipitated the drug rapidly after a few hours. This occurs because below the critical micellar concentration (CMC), micelle structure breaks down. Increasing Soluplus® above its CMC (7.6 mg/l in water) maintains micelle stability, enhances drug solubility and bioavailability for oral and parenteral administration, and prevents premature drug precipitation by ensuring micelle integrity is retained throughout the intended shelf life [42]. As in F3 (1:8) and F4 (1:10), the particle size is within in Nano-size (77 nm and 57 nm, respectively), as shown in table 2 [27].

For formulas F5 to F10, using TPGS as a copolymer with Soluplus® yields varying results based on TPGS content. At low TPGS content (F5 and F6), MTZ precipitates efficiently. In F7 (MTZ: Soluplus®:TPGS 1:8:2) and F8 (1:8:4), where Soluplus® remains constant, TPGS addition results in particle sizes of 77 nm and 78 nm, comparable to those observed with Soluplus® alone at similar ratios. For F9 (MTZ: Soluplus®:TPGS 1:6:4) and F10 (1:6:6), particle sizes are 71 nm and 77 nm, forming stable nanomicelles. Comparing F2, which contains only Soluplus® at the same ratio (MTZ: Soluplus® 1:6), indicates that TPGS enhances nanomicelle stability [28]. TPGS works as both a stabilizer and a solubilize; its amphiphilic structure promotes micelle formation and stability [29].

For Solutol HS, mixed soluplus® nanomicelles were a more stable preparation, even with a lower ratio of soluplus, strong hydrophobic interactions between soluplus® and Solutol HS, resulting in compact spherical micelles. Upon statistical analysis by compression F4 with other formulas, the P value< 0.05, which suggests there is a significant difference in particle size.

The polydispersity index (PDI) indicates the range of the particle size distribution. A PDI number approaching zero signifies a reasonably uniform particle size distribution, whereas a value

around one denotes a highly polydispersed distribution. The PDI of the prepared formula was close to zero, mean ingoing uniform distribution. The entrapment efficiency (EE) ranges from 85%to 90%, as shown in table (2). Our results show that as the concentration of soluplus® increases, the entrapment efficacy increases, as shown in the optimum formula F4, where, where the EE was 90%. Drug loading ranged from 7%to 10.08%.

Depend on data provide by particle size, EE%, DL% and pdI. the optimum formula was F4 (MTZ: soluplus®) in (1:10) weight ratio; that formula well undergo further investigation zeta potential, FTIR, DSC and FESEM.

Zeta potential prevents aggregation, as particles are repelled from each other by their surface charge, and it was equal to-7.10 mV, which is attributed to the non-ionic nature of the polymers used to develop the formulation [30].

The drug release profile for soluplus® nanomicelles F3 and F4 shows a similar release profile with an *f2* value of 75, which is more than 50, as shown in fig. 1. Nanomicelles prepared by a mixed polymer of soluplus® and TPGs (F9 and F10) show a similar release profile and enhancement in the release of MTZ; the *f2* value of the comparison of F9 and F10 versus the drug is less than 50, as shown in fig. 2. When comparing this formula with F4, they show *f2* equal to 35, which mean the release profile of MTZ of F4 is better than F9 and F10. The *f2* value for Soluplus®: Solutol HS nanomicelles versus the drug shows a dissimilar release profile as shown in fig. 3, and when compared with F4, it shows both of them with an *f2* value equal to 43, which means F4 has a great release profile.

The Fourier transform infrared spectroscopy (FTIR) fig. 4 shows characteristic MTZ peaks at 3439 cm^{-1} relative to N-H stretching, a band for the methyl group attached to the N_2 atom at 2931 cm^{-1}, and bands for the stretching of C-C of the phenyl group at 1587 cm^{-1} and 1450 cm^{-1}. The primary aromatic amines with N directly attached to the ring exhibit bands at 1336 cm^{-1} and 1253 cm^{-1}. The benzene ring C-H appears in the ranges of 1359 cm^{-1} to 1074 cm^{-1} that are accepted with references [31, 32].

The FTIR spectra of Soluplus® (fig. 5) has a distinctive peak for a hydroxyl group at 3437 cm^{-1} (O-H stretching). The peaks at 1741 cm^{-1} and 1633 cm^{-1} resemble the C=O stretching of the ester group and the tertiary amide group, respectively [33, 34].

The FTIR analysis of the selected formula shown in fig. 7 demonstrated analogous absorption peaks, which suggests that it is highly compatible with polymers. This indicates that there was no significant chemical interaction between the excipients and the medication, thereby confirming the drug's stability throughout the formulation process [23-41]. Fig. 6 shows a physical mixture of MTZ and Soluplus® and shows no interaction of the drug with the polymer.

The differential scanning calorimetric (DSC) thermogram of pure MTZ showed an endothermic peak at 112.42 °C having an enthalpy of 143.2 J/g, as shown in fig. 9. These results are in agreement with the foregoing literature [35-39]. Soluplus® showed a broad endothermic peak at 55 °C [36, 37] (fig. 10). For the selected formula, the DSC thermogram shows the transition from crystalline to amorphous due to nanomicelle formation, as in fig. 12. The result demonstrated that MTZ was well dispersed in the nanomicelles as an amorphous form [24-40].

CONCLUSION

Drug-loaded Soluplus® micelles alone and in combination, firstly with TPGS and secondly with Solutol HS 15 were prepared by the thin-film hydration method to prepare stable nanomicelles; their characterization of the optimum formula showed a mean size lower than 100 nm and PDI showed uniform distribution of particle size and enhancement in the *in vitro* release of the MTZ.

FUNDING

Nil

ACKNOWLEDGMENT

The authors would like to thank the College of Pharmacy, University of Baghdad, for their support.

AUTHORS CONTRIBUTIONS

Ahmed Ibrahim Ahmed-Design and conceptualization of work, performed the work, analyzed the data, Nawal Ayash Rajab–Analysis of the data and manage of experimental work.

CONFLICT OF INTERESTS

Declared none

REFERENCES

1. Hatamipour M, Sahebkar A, Alavizadeh SH, Dorri M, Jaafari MR. Novel nanomicelle formulation to enhance bioavailability and stability of curcuminoids. Iran J Basic Med Sci. 2019;22(3):282-9. doi: 10.22038/ijbms.2019.32873.7852, PMID 31156789.
2. Ezealisiji KE, Mbah CJ, Osadebe PO. Aqueous solubility enhancement of mirtazapine: effect of cosolvent and surfactant. Phamacology Pharmacy. 2015;6(10):471-6. doi: 10.4236/pp.2015.610049.
3. Ghalehkhondabi V, Soleymani M, Fazlali A. Folate-targeted nanomicelles containing silibinin as an active drug delivery system for liver cancer therapy. J Drug Deliv Sci Technol. 2021 Aug;61:102157. doi: 10.1016/j.jddst.2020.102157.
4. Mohamed S, Parayath NN, Taurin S, Greish K. Polymeric nano-micelles: versatile platform for targeted delivery in cancer. Ther Deliv. 2014;5(10):1101-21. doi: 10.4155/tde.14.69, PMID 25418269.
5. Razif MR, Chan SY, Widodo RT, Chew YL, Hassan M, Hisham SA. Optimization of a luteolin-loaded TPGS/Poloxamer 407 nanomicelle: the effects of copolymers hydration temperature and duration and freezing temperature on encapsulation efficiency particle size and solubility. Cancers (Basel). 2023;15(14):3741. doi: 10.3390/cancers15143741.
6. Pignatello R, Corsaro R, Bonaccorso A, Zingale E, Carbone C, Musumeci T. Soluplus® polymeric nanomicelles improve solubility of BCS-class II drugs. Drug Deliv Transl Res. 2022;12(8):1991-2006. doi: 10.1007/s13346-022-01182-x, PMID 35604634.
7. Shelake PR, Shah RR, Nalawade VV, Majalekar PP. Formulation and evaluation of solid self-emulsifying drug delivery system for drug mirtazapine. Int J Pharm Sci Res. 2019;10(10):934. doi: 10.13040/IJPSR.0975-8232.10.
8. Hamed HE, Hussein AA. Preparation *in vitro* and ex-vivo evaluation of mirtazapine nanosuspension and nanoparticles incorporated in orodispersible tablets. Iraqi J Pharm Sci. 2020;29(1):62-75. doi: 10.31351/vol29iss1pp62-75.
9. Aldeeb RA, Mahdy MA, El Nahas HM, Musallam AA. Design of mirtazapine solid dispersion with different carriers systems: optimization *in vitro* evaluation and bioavailability assessment. Drug Deliv Transl Res. 2023;13(9):2340-52. doi: 10.1007/s13346-023-01316-9, PMID 36940079.
10. Sulaiman HT, Rajab NA. Preparation and characterization of olmesartan medoxomil-loaded polymeric mixed micelle nanocarrier. Iraqi J Pharm Sci. 2024;33(4SI):89-100. doi: 10.31351/vol33iss(4SI)pp89-100.
11. Jassem NA, Abd Alhammid SN. Formulation and evaluation of canagliflozin self-nanomicellizing solid dispersion based on rebaudioside a for dissolution and solubility improvement. Iraqi J Pharm Sci. 2024;33(4SI):43-56. doi: 10.31351/vol33iss(4SI)pp43-56.
12. Al wiswasi NN, Al Gawahri FJ. Brimonidine soluplus nanomicelles: preparation and *in vitro* evaluation. Iraqi J Pharm Sci. 2025;34(1):246-55. doi: 10.31351/vol34iss1pp246-255.
13. Mohammed AA. Preparation *in vitro* evaluation and characterization studies of clozapine nanosuspension. 2025;33(4SI):336-48. doi: 10.31351/vol33iss(4SI)pp336-348.
14. Rashid AM, Ghareeb MM. Using ionic liquid-based surfactant in formulating nimodipine polymeric nanoparticles: a promising approach for improved performance. Iraqi J Pharm Sci. 2025;34(1):203-17. doi: 10.31351/vol34iss1pp203-217.
15. Al Edhari GH, Al Gawhari FJ. Study the effect of formulation variables on preparation of nisoldipine-loaded nano bilosomes. IJPS. 2023;32Suppl:271-82. doi: 10.31351/vol32issSuppl.pp271-282.
16. Radhi AA, Ali WK, Al Saedi F. Preparation and *in vitro* evaluation of synthetic high-density lipoproteins as parenteral drug delivery system for tamoxifen citrate. IJPS. 2023;32(3):105-17. doi: 10.31351/vol32iss3pp105-117.

17. Keshari P, Sonar Y, Mahajan H. Curcumin-loaded TPGS micelles for nose-to-brain drug delivery: *in vitro* and *in vivo* studies. Mater Tech Internet. 2019;34(7):423-32. doi: 10.1080/10667857.2019.1575535.
18. El Helaly SN, Rashad AA. Mirtazapine loaded polymeric micelles for rapid-release tablet: a novel formulation-*in vitro* and *in vivo* studies. Drug Deliv Transl Res. 2024;14(9):2488-98. doi: 10.1007/s13346-024-01525-w, PMID 38353837.
19. Rashid AM, Abdal Hammid SN. Formulation and characterization of itraconazole as nanosuspension dosage form for enhancement of solubility. Iraqi J Pharm Sci. 2019;28(2):124-33. doi: 10.31351/vol28iss2pp124-133.
20. Abdulqader AA, Sultan NA. Preparation and characterization of posaconazole as a nano-micelles using d-α-tocopheryl polyethylene glycol 1000 succinate (TPGS). Iraqi J Pharm Sci. 2023;32Suppl:26-32. doi: 10.31351/vol32issSuppl.pp26-32.
21. Salih O, Muhammed E. Preparation, evaluation and histopathological studies of ondansetron-loaded invasomes transdermal gel. J Res Pharm. 2024;28(1):289–303. doi: 10.29228/jrp.696.
22. Salih OS, Hamoddi ZM, Taher SS. Development and characterization of controlled release tablets of candesartan cilexetil/ β-cyclodextrin inclusion complex. Int J Drug Deliv Technol. 2020;10(2):273-83. doi: 10.25258/ijddt.10.2.15.
23. De Groat W, Abdelhalim H, Patel K, Mendhe D, Zeeshan S, Ahmed Z. Discovering biomarkers associated and predicting cardiovascular disease with high accuracy using a novel nexus of machine learning techniques for precision medicine. Sci Rep. 2024;14(1):1. doi: 10.1038/s41598-023-50600-8, PMID 38167627.
24. Arukkunakorn W, Sajomsang W, Ovatlarnporn C. Resveratrol enhance loading capacity and solubility of dimethylcurcumin in pluronic f-127 nanomicelles. Eur Chem Bull; 2023 July.
25. Nalinbenjapun S, Sripetthong S, Basit A, Suksuwan A, Sajomsang W, Ovatlarnporn C. Fabrication of curcumin-loaded nano-micelles based on quercetin-quarternary ammonium-chitosan (Qu-QCS) conjugate and evaluation of synergistic effect with doxorubicin against breast cancer. Int J Biol Macromol. 2024;281(2):135904. doi: 10.1016/j.ijbiomac.2024.135904, PMID 39482127.
26. Brandao FC, Tagiari MP, Silva MA, Berti LF, Stulzer HK. Physical-chemical characterization and quality control of spironolactone raw material samples. Pharm Chem J. 2008;42(6):368-76. doi: 10.1007/s11094-008-0129-3.
27. Piazzini V, D Ambrosio M, Luceri C, Cinci L, Landucci E, Bilia AR. Formulation of nanomicelles to improve the solubility and the oral absorption of silymarin. Molecules. 2019;24(9):1688. doi: 10.3390/molecules24091688, PMID 31052197.
28. Ali R, Qamar W, Kalam MA, Binkhathlan Z. Soluplus-TPGS mixed micelles as a delivery system for brigatinib: characterization and *in vitro* evaluation. ACS Omega. 2024;9(40):41830-40. doi: 10.1021/acsomega.4c06264, PMID 39398132.
29. Miyazawa T, Itaya M, Burdeos GC, Nakagawa K, Miyazawa T. A critical review of the use of surfactant-coated nanoparticles in nanomedicine and food nanotechnology. Int J Nanomedicine. 2021;16:3937-99. doi: 10.2147/IJN.S298606, PMID 34140768.
30. Shakiba E, Khazaei S, Hajialyani M, Astinchap B, Fattahi A. Preparation and *in vitro* characterization of retinoic acid-loaded poly(ε-caprolactone)-poly(ethylene glycol)-poly(ε-caprolactone) micelles. Res Pharm Sci. 2017;12(6):465-78. doi: 10.4103/1735-5362.217427, PMID 29204175.
31. Musallam AA, Mahdy MA, Elnahas HM, Aldeeb RA. Optimization of mirtazapine loaded into mesoporous silica nanostructures via box-behnken design: *in vitro* characterization and *in vivo* assessment. Drug Deliv. 2022;29(1):1582-94. doi: 10.1080/10717544.2022.2075985, PMID 35612286.
32. Circioban D, Ledeți A, Ridichie A, Vlase T, Ledeți I, Bradu IA. Compatibility study of mirtazapine with several excipients used in pharmaceutical dosage forms employing thermal and non-thermal methods. J Therm Anal Calorim. 2024;150(9):6747-59. doi: 10.1007/s10973-024-13181-w.
33. Alwan RM, Rajab NA. Nanosuspensions of selexipag: formulation characterization and *in vitro* evaluation. Iraqi J Pharm Sci. 2021;30(1):144-53. doi: 10.31351/vol30iss1pp144-153.
34. Lan Y, Ali S, Langley N. Characterization of Soluplus® by FTIR and raman spectroscopy. In: Proceedings of the CRS 2010 Annual Conference; 2010 Oct. p. 1138.
35. Naresh WR, Dilip DV, Sunil KP. Xyloglucan-based nasal in situ gel formulation of mirtazapine for treatment of depression. Indian J Pharm Educ Res. 2020;54(2 Suppl):S210-9. doi: 10.5530/ijper.54.2s.77.
36. Pawar JN, Shete RT, Gangurde AB, Moravkar KK, Javeer SD, Jaiswar DR. Development of amorphous dispersions of artemether with hydrophilic polymers via spray drying: physicochemical and in silico studies. Asian J Pharm Sci. 2016;11(3):385-95. doi: 10.1016/j.ajps.2015.08.012.
37. Shamma RN, Basha M. Soluplus®: a novel polymeric solubilizer for optimization of carvedilol solid dispersions: formulation design and effect of method of preparation. Powder Technol. 2013;237:406-14. doi: 10.1016/j.powtec.2012.12.038.
38. Marimuthu A, Seenivasan R, Pachiyappan JK, Nizam I, Ganesh G. Synergy of science and tradition: a nanotechnology-driven revolution in natural medicine. Int J App Pharm. 2024;16(6):10-20. doi: 10.22159/ijap.2024v16i6.50767.
39. Nafis FDR, Sriwidodo, Chaerunisaa AY. Study on increasing solubility of isolates: methods and enhancement polymers. Int J Appl Pharm. 2022;14(6):6-13. doi: 10.22159/ijap.2022v14i6.45975.
40. Alkufi HK, Kassab HJ. Soluplus stabilized nimodipine entrapped Spanlastic formulations prepared with edge activator (Tween20): comparative physicochemical evaluation. Pharm Nanotechnol. 2024;13(3):551-63. doi: 10.2174/0122117385348551241028102256, PMID 39501952.
41. Alkufi HK, Kassab HJ. Nanospanlastic in situ gel for nose to brain delivery of nimodipine: *in vitro* optimization and *in vivo* pharmacokinetic study. Al Rafidain J Med Sci. 2025;8(1):97-105. doi: 10.54133/ajms.v8i1.1687.
42. Guembe Michel N, Nguewa P, Gonzalez Gaitano G. Soluplus®-based pharmaceutical formulations: recent advances in drug delivery and biomedical applications. Int J Mol Sci. 2025;26(4):1499. doi: 10.3390/ijms26041499, PMID 40003966.